minerals

MDPI

Article

Influences of CO_2 on the Microstructure in sheared olivine Aggregates

Huihui Zhang [1,3], Ningli Zhao [2], Chao Qi [1], Xiaoge Huang [1,*] and Greg Hirth [2]

[1] Institute of Geology and Geophysics, Chinese Academy of Sciences, Beijing 100029, China; zhanghuihui@mail.iggcas.ac.cn (H.Z.); qichao@mail.iggcas.ac.cn (C.Q.)
[2] Department of Earth, Environmental and Planetary Sciences, Brown University, Providence, RI 02906, USA; ningli_zhao@brown.edu (N.Z.); greg_hirth@brown.edu (G.H.)
[3] University of Chinese Academy of Sciences, Beijing 100049, China
* Correspondence: xghuang@mail.iggcas.ac.cn; Tel.: +010 82998429

Appendix A

Contents of this file: Appendix Figures A1 to A4; Tables A1

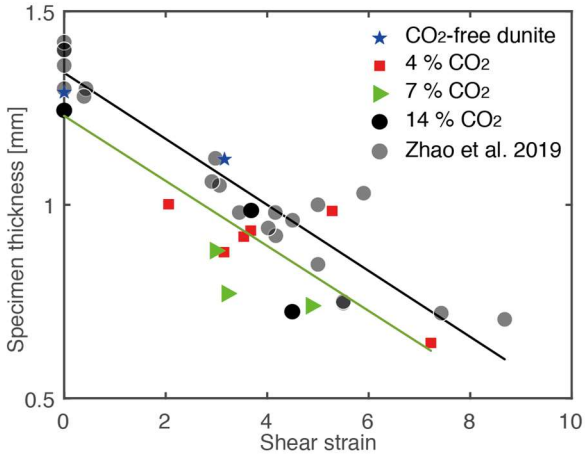

Figure A1. The thickness of the specimens as a function of the shear strain. The result includes data from different CO_2 contents (4 %, 7 %, 14 %) and CO_2-free dunite. Gray circles are data from Zhao et al. [1]. The green line is a least square fit to data from this work; the black line is a least square fit to the data from Zhao et al. [1].

Water contents in the polycrystalline aggregates were determined by Fourier transform infrared (FTIR) spectroscopy in transmission. To calculate hydroxyl concentration, we integrated spectra between 3650 cm^{-1} and 3000 cm^{-1}, which covered infrared hydroxyl stretching bands for Ol, CPx, and OPx [1–4].

We examine the hot-pressed sample to obtained water contents that the thickness of the sample wafer was 0.3 mm. The polycrystal of the hot-pressed sample (including grain boundaries) contained ~9 ppm H_2O by weight (~150 H/10^6 Si), indicate that olivine aggregates are anhydrous prepared through this procedure. FTIR results are presented in Figure A2.

Citation: Lastname, F.; Lastname, F.; Lastname, F. Title. *Minerals* **2021**, *11*, x. https://doi.org/10.3390/xxxxx

Academic Editor: Firstname Lastname

Received: date
Accepted: date
Published: date

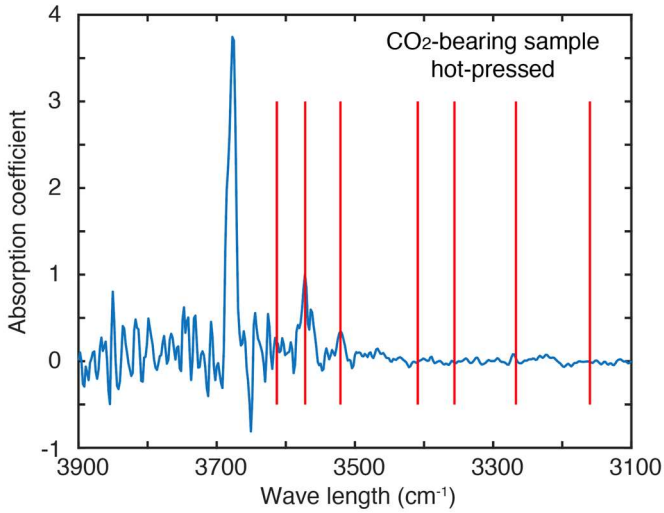

Figure A2. FTIR spectra from hot-pressed polycrystalline sample (W2261). The characteristic OH stretching bands in Ol (3613, 3572, 3521, 3409, 3356, 3267, 3160 cm^{-1}) were presented by solid red lines.

At our experiment condition (1 GPa and 1100ºC), the system of Ol + CPx + CO_2 remains stable according to the solidus curve [5,6]. EMPA shows the composition of the starting sample and deformed sample. The results of Table A1 show the composition of the dark gray melt in Figures 2a and 2b and the light gray melt at Figure 2b, and the light gray melt between sample and piston (Figure A3). Images of Figure A3 obtained from initial sample not etched. According to Table A1, the light hollow on triple junctions is the Ca-rich carbonate melt and the anomalous dark mineral is the Mg-rich carbonate melt. From A3(a) and (b), the melt was aggregated to the boundary of the sample according to the EDS result (Ca).

Table A1. Summary of the EPMA

No.	CaO	MgO	FeO	SiO2	Al2O3	Cr2O3	TiO2	Na2O	K2O	MnO	NiO	CO2	Total	Comment
W2261-light[1]-gray-melt	48.17	7.21	1.54	5.84	0.00	0.00	0.00	0.01	0.01	0.03	0.05	37.17	100.00	Hot-pressed specimen
W2261-dark[2]-gray-melt	1.17	36.89	5.88	5.66	0.03	0.00	0.03	0.05	0.00	0.08	0.14	50.08	100.00	Hot-pressed specimen
W2264-dark[3]-gray-melt	1.42	45.45	7.75	38.42	0.60	0.20	0.02	0.03	0.00	0.09	0.37	5.64	99.99	Deformed specimen
W2264-light[4]-gray-melt	23.98	19.99	2.13	48.93	6.30	0.02	0.09	0.10	0.00	0.04	0.13	0.00	101.75	Deformed specimen
Dolomite	34.40	23.08	0.02	-0.09	0.00	0.01	-0.01	0.00	0.01	0.00	-0.02	42.28	99.88	Dolomite
W2261-olivine	0.13	49.24	8.60	40.04	0.01	0.02	0.02	-0.01	-0.01	0.13	0.43	1.34	99.96	Hot-pressed specimen
W2261-diopside	13.34	30.36	5.12	47.19	3.14	0.40	0.37	0.27	0.00	0.12	0.19	0.00	100.49	Hot-pressed specimen

light[1]: is the light triple junctions of Figure 2(b).
dark[2]: is the dark gray melt of Figure 2(a) and 2(b).
dark[3]: is the dark gray melt of deformed sample not etched.
light[4]: is the light gray melt between sample and piston of Figure A3(c).

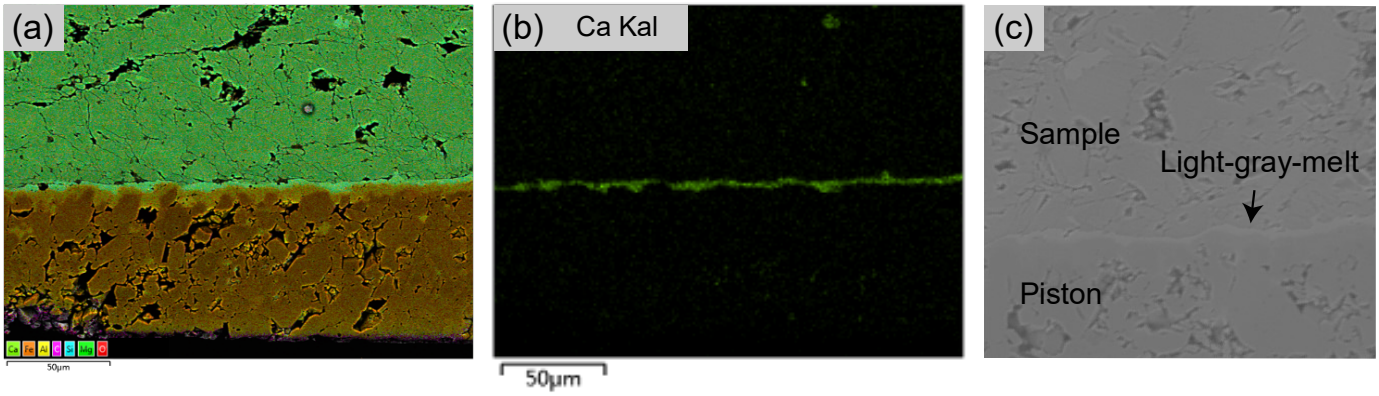

Figure A3. The sample section for the deformed sample (W2264, not etched). (a) and (b) The energy-dispersive X-ray spectroscopy (EDS). (c) A BSE image. The composition of light-gray-melt was analyzed by EPMA.

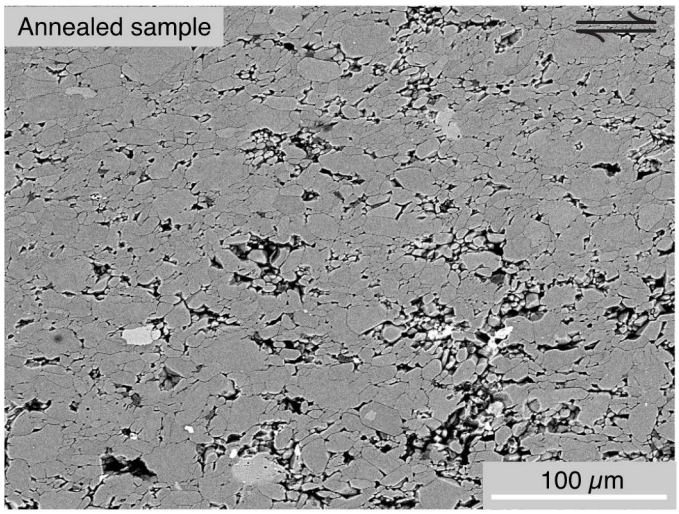

Figure A4. The BSE image of the annealed sample (W2266) with etched.

References

1. Zhao, N.; Hirth, G.; Cooper, R.F.; Kruckenberg, S.C.; Cukjati, J. Low viscosity of mantle rocks linked to phase boundary sliding. *Earth and Planetary Science Letters* **2019**, *517*, 83–94, doi:10.1016/j.epsl.2019.04.019.
2. Berry, A.J.; Hermann, J.; O'Neill, H.S.C.; Foran, G.J. Fingerprinting the water site in mantle olivine. *Geology* **2005**, *33*, 869–872, doi:10.1130/G21759.1.
3. Demouchy, S.; Ishikawa, A.; Tommasi, A.; Alard, O.; Keshav, S. Characterization of hydration in the mantle lithosphere: Peridotite xenoliths from the Ontong Java Plateau as an example. *Lithos* **2015**, *212–215*, 189–201, doi:10.1016/j.lithos.2014.11.005.
4. Ferriss, E.; Plank, T.; Walker, D. Site-specific hydrogen diffusion rates during clinopyroxene dehydration. *Contributions to Mineralogy and Petrology* **2016**, *171*, 1–24, doi:10.1007/s00410-016-1262-8.
5. Wyllie, P.J.; Huang, W.L. Influence of mantle CO2 in the generation of carbonatites and kimberlites. *Nature* **1975**, *257*, 297–299, doi:10.1038/257297a0.
6. Dalton, J.A.; Presnall, D.C. Carbonatitic melts along the solidus of model lherzolite in the system CaO-MgO-Al2O3-SiO2-CO2 from 3 to 7 GPa. *Contributions to Mineralogy and Petrology* **1998**, *131*, 123–135, doi:10.1007/s004100050383.